

NUMERICAL STUDY OF LANDER ENGINE PLUME IMPINGEMENT ON THE SURFACE OF EUROPA

Rebekah Lam[^], Elham Maghsoudi⁺, William Hoey^{*}

Plume exhaust from lander engines would be of concern when landing on the surface of Europa since it could have detrimental effects on both the landing surface and powered descent vehicle. The plume could also entrain particles and redirect them up toward the landing vehicle, as well as erode and contaminate the surface where science would be conducted. In this work, a numerical methodology is developed and validated to conduct a first-order assessment of individual engine plumes of a potential Europa Lander vehicle. Computational Fluid Dynamics (CFD) is used to solve the flow field inside and immediately downstream of the nozzle, while the Direct Simulation Monte Carlo (DSMC) method is applied further downstream where the flow becomes rarefied. An interface between the two domains is defined where macroscopic flow data is passed from the CFD domain to the DSMC domain, establishing a one-way coupling. Plume pressure and velocity fields, as well as ground heating, pressure and density flux profiles, are obtained at altitudes from 25 m down to 10 m, spanning the final stages of landing. The codes and methodologies used in this study are successfully validated with simulations conducted by Morris et al. [1-3] of the Apollo Lunar Module Descent Engine (LMDE) exhaust plume impinging onto the lunar surface.

NOMENCLATURE

c_p :	Specific heat, J/kg.K
L :	Flow Characteristic Length, m
M_0 :	Molecular Weight, g/mole
r :	Radial distance from axis of symmetry
R :	Gas Constant, J/mole.K
r/D :	Dimensionless radial distance from the axis of symmetry
y/D :	Dimensionless axial distance from the nozzle exit plane
T :	Translational Temperature, K
Kn :	Dimensionless Knudsen Number
λ :	Mean Free Path, m
γ :	Ratio of Specific Heat
μ :	Dynamic Viscosity, Pa.sec
ρ :	Density, kg/m ³

I. INTRODUCTION

It is important to assess lander engine plume interactions with the European surface for several reasons. Direct impingement of the gas plume on a lander during its descent can cause torques, contamination and heating on the surfaces of the vehicle, all of which must be well-characterized to aid in the design of the landing vehicle. Further, particles may be removed from the European surface by the

[^]Propulsion Engineer, NASA Jet Propulsion Laboratory California Institute of Technology, Rebekah.L.Lam@jpl.nasa.gov

⁺AeroThermo Engineer, NASA Jet Propulsion Laboratory California Institute of Technology, Elham.Maghsoudi@jpl.nasa.gov

^{*} Contamination Control engineer, NASA Jet Propulsion Laboratory California Institute of Technology, William.A.Hoey@jpl.nasa.gov

high-pressure, high-velocity plume flow and redirected up toward the descent stage, where instruments sensitive to particulate contamination – such as Light Detection and Ranging (LIDAR) sensors and cameras – can be affected during descent. Morris et al. modelled the entrainment and spray of lunar surface particles by a lander engine plume in a similarly rarefied environment [1-3]. Additionally, since a lander would need to collect surface samples from its immediate vicinity, it is essential to know if the plume has eroded the surface or contaminated it with engine exhaust products such as ammonia. Ammonia is of particular concern to Europa astrobiology missions where any nitrogenous deposits from the engine plume could affect the search for likely small traces of nitrogen compounds as biomarkers or habitability indicators [4]. A significant effort can be made to study each of the aforementioned plume concerns, however, this study takes the first step in assessing the surface plume impingement from a single lander engine.

Mars missions typically apply Computational Fluid Dynamics (CFD) to simulate entire plume flows from engines down to the ground [5]. The continuum assumption is valid for Mars background pressure and CFD code can be used to resolve the flow field. However, in environments such as that of Europa where plume flows expand into a nearly-collisionless vacuum, continuum models eventually become invalid and rarefied gas dynamic techniques like Direct Simulation Monte Carlo (DSMC) are required [1-3,6]. Within a simulation domain, the transition from CFD to DSMC techniques must occur before the flow becomes sufficiently rarefied; however, this transition should occur as far downstream as possible, since highly collisional flow is computationally expensive for DSMC.

In this study, a hydrazine monopropellant engine is selected as a candidate for the potential Europa lander engine, as is consistent with the study done by Hand et al. [7]. Exhaust plume of the selected nozzle is modelled in a three-step approach. First, a 2D axisymmetric model of the nozzle is built. Flow inside and just downstream of the nozzle is solved using CFD where the continuum assumption is valid and flow beyond that, in the rarefied region, is solved using DSMC. A CFD/DSMC transition interface is established based on a non-dimensional Knudsen number, Kn , flow direction and interface-normal Mach number. Here, the CFD flow field data is manually passed to the DSMC model as an inflow boundary. Then the full plume flow field extending to the surface is modelled in the DSMC domain. The commercial package STAR-CCM+ is used for CFD and NASA's DSMC Analysis Code, DAC [6] is used for DSMC. Both STAR-CCM+, and DAC are validated using simulations of the Apollo Lunar Module Descent Engine (LMDE) plume conducted by Morris et al. [1-3], as demonstrated herein. Although a potential Europa Lander mission would use four pairs of 5 and 30 degree nozzles [7], single nozzles were modelled in this study as a preliminary assessment. Resulting flow fields and surface profiles at altitudes spanning the approximate final stages of descent of the potential mission, from 25 m to a minimum of 10 m [7], are discussed.

II. LANDER ENGINE CFD SIMULATIONS

A Non-reacting Eulerian multi-component gas model with real gas assumption is used in STAR-CCM+ to solve this problem numerically, taking into account all the main exhaust plume species. Coupled Flow and coupled energy are used to solve Navier Stokes and Energy equations to resolve the flow field and temperature in the CFD domain. Simulations were initially solved using a constant specific heat assumption; however, the LMDE validation study proved the importance of using a temperature-dependent specific heat (c_p). While adjusting the specific heat to a constant value gives good agreement in a specific location of the flow field with corresponding temperature to that specific heat, it can cause errors as large as 30% in other locations. Specific heat variations with temperature shows significant changes in the temperature profile within the nozzle and the far-field. Final results are obtained with temperature-dependent specific heat profiles for each of the species. The K-Omega turbulence model is used and the mesh is refined to achieve Y^+ of 1 at the nozzle walls.

Flow field and temperature are solved in the domain for a 3D wedge model, and then the model is reduced to a 2D axisymmetric domain to reduce the computational time. The pressure and temperature

[Type here]

data of the resolved solution at the exit plane and inside the nozzle are compared to that of the wedge model for validation. A mesh independence study is completed to achieve the coarsest cell size at which results are not mesh dependent.

A back pressure sensitivity analysis is completed for CFD for pressures as low as 50 Pa. No significant change at the exit plane and CFD/DSMC interface is observed as the back pressure is reduced below 600 Pa.

A dimensionless Knudsen number is used to determine where to define the boundary between CFD and DSMC solutions, and to what extent the near-nozzle domain may be well-modeled as continuum. The Knudsen number is defined as the ratio of mean free path, λ , to flow characteristic length, L , and may be expressed as:

$$\text{Kn} = \frac{\lambda}{L} = \frac{\mu}{\rho L} \sqrt{\frac{\pi M_0}{2RT}}, \quad \text{Eq. 1}$$

for a single-species mixture where μ represents the flow dynamic viscosity, ρ the density, M_0 the molecular weight, R the gas constant, and T the translational temperature. A local dimensionless Knudsen number is defined in Eq. 2 by substituting the density gradient length scale for L :

$$\text{Kn} = \frac{\mu}{\rho^2} \sqrt{\frac{\pi M_0}{2RT}} |\nabla \rho|. \quad \text{Eq. 2}$$

Continuum models of fluid dynamics are valid for Knudsen numbers smaller than 10^{-3} [8]. As Kn increases in a flow, e.g. as density decreases, intermolecular collisions grow infrequent and viscous stress and heat flux can no longer be defined in terms of gradients of continuous flow properties. As mean free paths grow to exceed scale lengths, i.e. at $Kn \gg 1$, molecules almost never collide amongst themselves and instead propagate ballistically in a free-molecular ‘flow’ regime.

A Kn contour plot is used in the lander plume simulation domain to determine where the transition to rarefied flow occurs. Two criteria are considered to define this CFD/DSMC interface and its configuration, consistent with Morris et al. [1-3]:

- An interface at which Kn numbers are smaller than 0.001 (10^{-3})
- Flow normal to the interface should be supersonic

A CFD/DSMC interface optimization study is conducted to define an interface within the continuum regime as far as possible from the nozzle to avoid generating a highly-collisional (and therefore computationally-expensive) DSMC flow, while simultaneously being of appropriate configuration to keep flow supersonic normal to the interface surface. This process is discussed in more depth in Section V and the resulting DSMC flow fields are shown there as well.

III. CFD VALIDATION

In order to validate the commercial CFD code, STAR-CCM+, the Apollo Lunar Module Descent Engine (LMDE) was simulated and results are compared with those from Aaron Morris’s LMDE simulations which applied NASA’s DPLR CFD code [1-3]. The LMDE nozzle shape is reproduced in STAR-CCM+, and an axisymmetric computational domain identical to that in Morris’s simulation was created, extending 10 m from the nozzle inlet to the ground and 5 m radially from the axis of symmetry. Identical nozzle boundary conditions are defined for a single-species flow of water vapor. The STAR-CCM+ simulation was initially conducted twice with constant ratios of specific heats (γ): at $\gamma = 1.20$ representing vapor properties at 2000 K, and $\gamma = 1.33$ representing vapor properties at 250 K. Ultimately, a simulation was conducted with specific heat as a function of temperature consistent with the definition by Morris [1], which allowed for the interpolation of γ as a function of temperature throughout the domain. These results show excellent agreement with Morris’s both inside and downstream of the nozzle, in the nearfield and farfield domain, as seen in Figure 1. Pressure perturbations seen in the right side of the

[Type here]

plume at the border of high-pressure dense region and low-pressure background are due to the numerical instabilities. Since the perturbations are outside of the area of the interest and downstream of where the CFD/DSMC interface will be drawn, the code is not run longer to get them resolved.

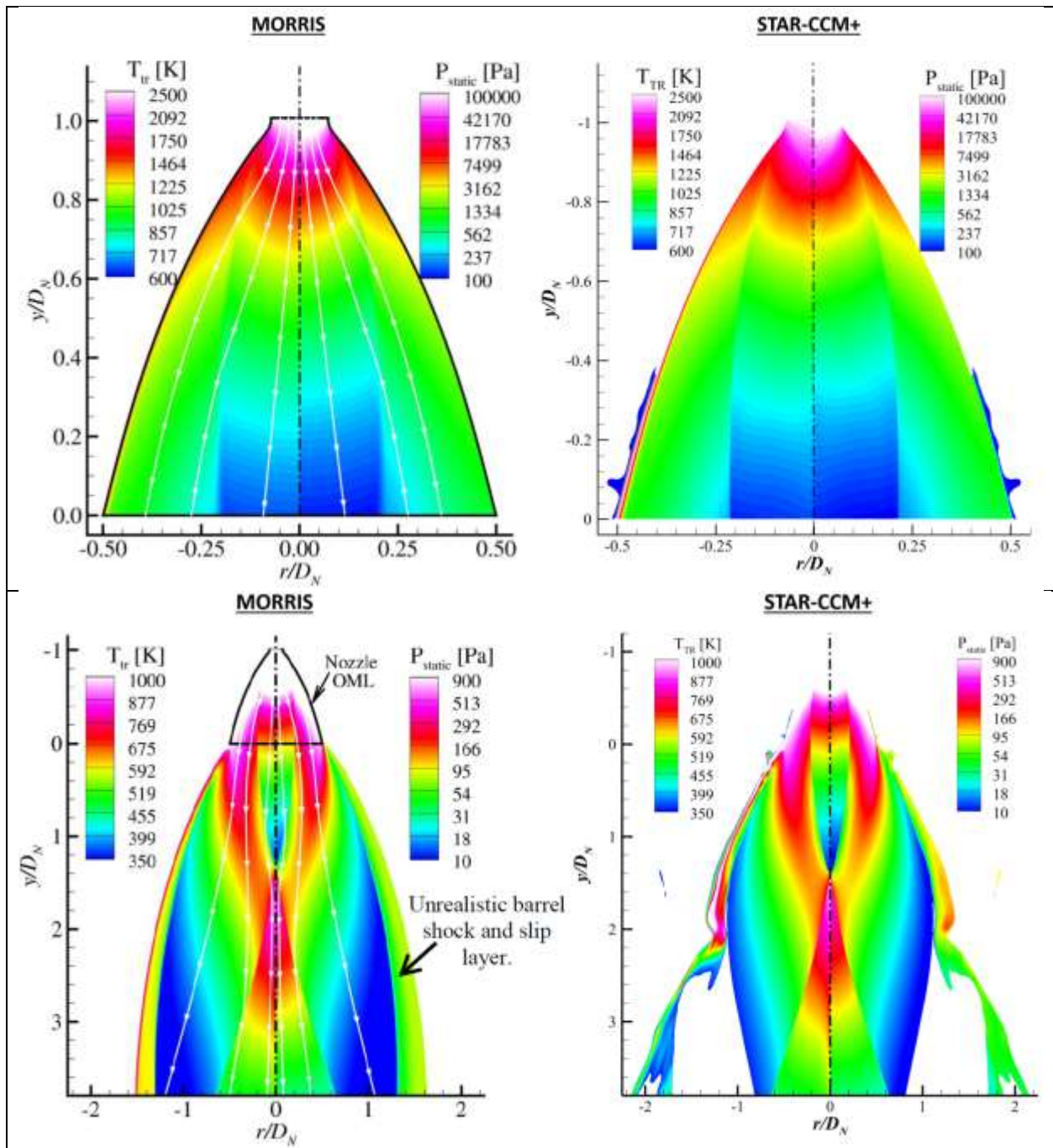


Fig. 1: Contours of translational temperature [K] and static pressure [Pa] on uniform color bars. At left: Morris [1]; at right: STAR-CCM+ with variable specific heat.

Vertical velocity, temperature and density of vapor are plotted at the nozzle exit plane in Figure 2. Results are shown to be in good agreement with Morris's simulations except for temperature and density right at the edge of the nozzle.

[Type here]

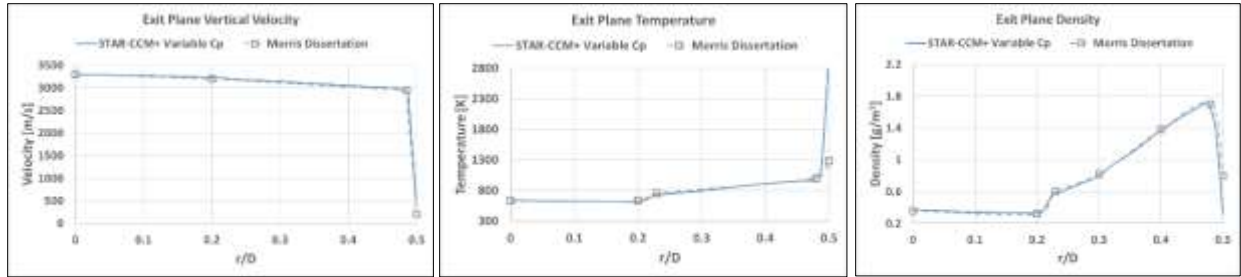


Fig. 2: LMDE nozzle exit plane results, STAR-CCM+ vs. Morris's dissertation [1].

IV. DSMC VALIDATION

The DAC code [6] is validated with the same LMDE plume study [1-3] used to validate the CFD code in Section III. Morris uses an in-house DSMC solver from The University of Texas at Austin, which is one-way coupled to NASA's Data Parallel Line Relaxation (DPLR) CFD code and also incorporates the ability to model two-phase flow for lunar dust entrainment [1-3]. Macroscopic properties from the validated STAR-CCM+ solution are obtained at the same CFD/DSMC interface used by Morris and used as inflow data in the DSMC simulation. This interface extends down axially from the outer edge of the nozzle to 3.25 nozzle diameters from the exit plane, then radially inward toward the axis, as shown in Figure 4. Ideally, the hybrid interface should be defined such that interface-normal flow is supersonic to prevent any backflow into the CFD domain. However, in this case, it is only supersonic on the radially aligned interface and close to the nozzle on the axially aligned interface. Morris makes a similar note on this, but considered it to be acceptable as there is good agreement between the CFD and DSMC results across this interface, because boundaries are "typically drawn where the flow is largely inviscid and flow gradients are weak." [1] Similarly, as shown in Figure 4, there is evident continuity from the STAR-CCM+ to DAC contours.

2D AXISYMMETRIC SIMULATIONS

Axisymmetric DAC simulations for the LMDE nozzle are run at altitudes of 20 m and 5 m, to compare to the results produced by Morris. Water vapor is used as the simulated fluid, with its associated molecular properties matching those used by Morris [1], and the wall boundary representing the lunar surface is set to a diffuse isothermal wall at 350 K. For simplicity, a uniform grid, with a layer of smaller cell sizes along each boundary is used. For the 20 m altitude, the domain extends 20 m in the radial direction and is made up of 1 cm cells, with 1.4 mm cells along the boundaries. For the 5 m altitude simulation, the domain extends 7 m in the radial direction and is made up of 0.5 cm cells, with 1.7 mm cells along the boundaries. This grid size intermittently exceeds the flow mean free path, primarily near the nozzle exit plane, along the symmetry axis, and far downstream from the surface shock. However, the grid is demonstrated to be sufficiently refined to everywhere resolve the gradient length scales of macroscopic flow properties (i.e. density and temperature).

The pressure contours produced by DAC in comparison to Morris's are shown in Figures 3 and 4. The general flow structure of both the 20 m and 5 m altitude LMDE plume in Morris's simulation is reproduced very well in DAC.

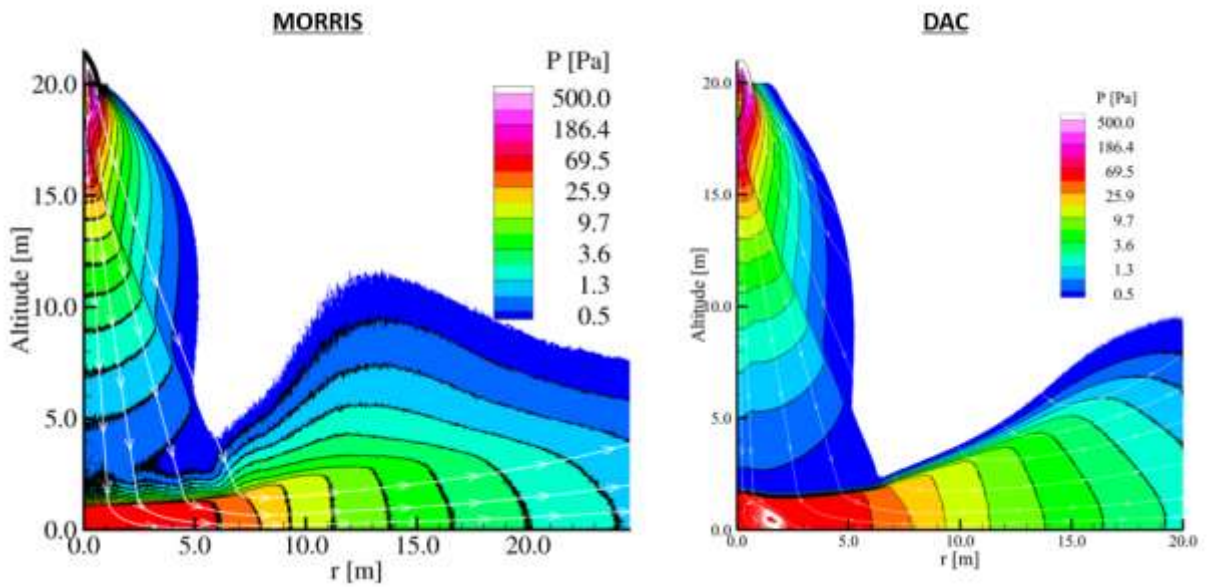


Fig. 3: Pressure Contour comparison to Morris [1] for 20 m altitude.

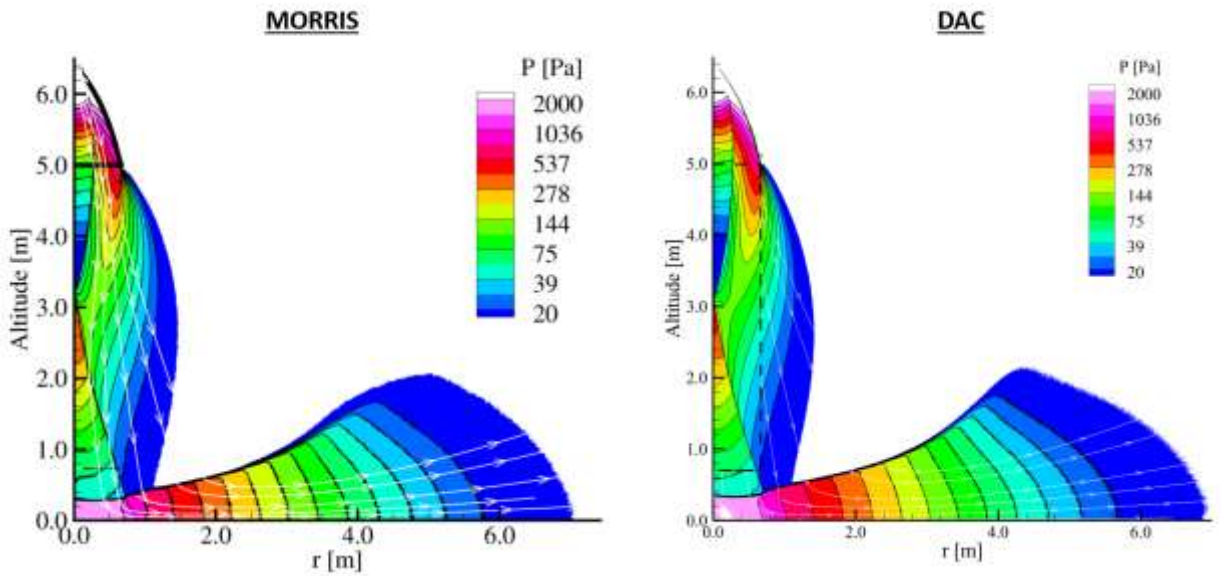


Fig. 4: LMDE pressure contour comparison to Morris [1] for 5 m altitude. CFD/DSMC Interface is shown as dashed line.

The surface shock standoff distance at the axis is about 1.5 m in the 20 m altitude DAC simulation and 0.34 m thick in the 5 m altitude DAC simulation, thinning as the engine descends. In the Morris simulations, the surface shock thicknesses decrease with altitude as well, but are slightly thinner, at about 1.0 m and 0.24 m respectively. This is likely due to the recirculation zone that exists in the DAC simulations. Simulations were tracked before averaging in both DAC simulations to observe the time-dependent behavior of such recirculation zones, and it was found that they were steady features. Morris

[Type here]

mentions a small recirculation zone at a 15m altitude, but does not discuss it for 20m or 5m [1]. The surface shocks in the DAC simulations also exhibit similar behavior to Morris's, as they stay almost parallel to the surface until they intersect with the reflected nozzle shock and are deflected slightly upward. This occurs at about 7.5 m from the axis in the 20 m simulation and 0.8 m in the 5 m simulation, slightly further out than in the Morris simulations where they deflect at 6 m and 0.75 m respectively. This again could be due to the recirculation zone in the DAC simulations. Lastly, the DAC simulation actually shows a much cleaner shock in the 20 m altitude case. Morris notes that a discretization issue could have caused the waviness of the surface shock in his simulation [1].

For the 5 m altitude, Morris also provides data on the ground heating profile. The same data is obtained in DAC and is shown with Morris's data in Figure 5, however only out to a radial distance of 7 m. The surface heating profiles compare very well, both peaking at about 0.5 m from the axis at about 300 to 400 kW/m² and both with a similar discontinuity at approximately $r = 1$ m.

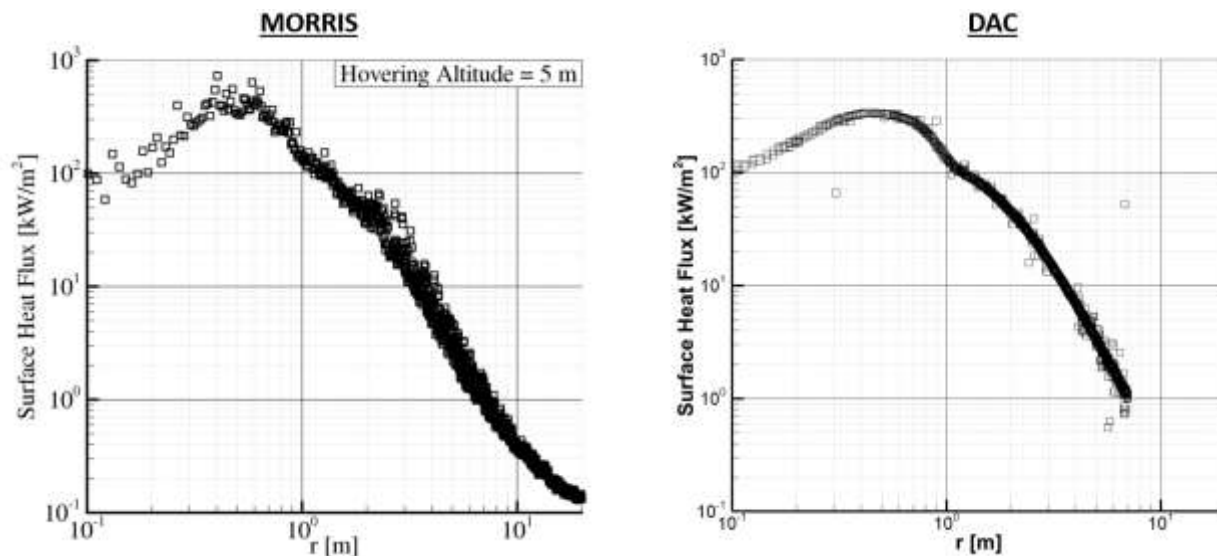


Fig. 5: LMDE plume surface heat flux comparison to Morris [1] at 5 m altitude

3D SIMULATIONS

Although there are minor differences, possibly due to differences in gridding and numerical weighting methods, the DAC code is validated well in the 2D axisymmetric case. However, one caveat to this validation is that for the potential Europa lander engine simulations, 3D models will be used since the nozzles are canted and therefore cannot be captured in an axisymmetric simulation. To further validate the DAC code, specifically with respect to its 3D capabilities, the 20 m and 5 m altitude cases were repeated with a 3D DSMC domain, employing a half symmetry of the nozzle. To obtain the 3D CFD/DSMC boundary, the axisymmetric CFD/DSMC interface is swept over 180 degrees to create a surface and the macroscopic flow properties are copied across this surface as well. An axisymmetric slice of this 3D result is then compared to the actual axisymmetric simulation result.

The grid for 3D simulations must be much coarser than the axisymmetric grids. The 20 m altitude simulation uses a base grid size of 3.3 cm, with cells as small as 1.4 cm along the ground. For the 5 m altitude, a base grid size of 2.5 cm is used, with 1.7 cm cells along the surface. These are the smallest reasonable grid sizes attainable and, as with the axisymmetric case, are small enough to resolve gradient length scales of macroscopic properties, so should yield accurate results.

The resulting 3D pressure contours generally match the axisymmetric contours well in both the 20 m and 5 m simulations. In the 20 m simulation, the recirculation zone near the axis exists and is roughly the same size as it is in the axisymmetric result. However, in the 5 m altitude case, the recirculation zone

[Type here]

does not exist in 3D. Future work could study the flow fields at intermediate altitudes to further investigate this discrepancy, however, it is less important to this study since the potential Europa lander nozzles are canted and the same recirculation zone should not form.

A comparison of the surface heating between the axisymmetric and 3D cases is shown in **Error! Reference source not found.** 6. In the 20 m case, the 3D simulation shows slightly higher heating than the axisymmetric case, but trends very similarly. In the 5 m case, **Error! Reference source not found.** the 3D heating is again similar in trend but considerably higher than the axisymmetric heating, especially near the axis, where it does not taper off as significantly between the peak value and the nozzle axis. This is because in the axisymmetric case, the recirculation zone appears to provide a cooling effect near the axis. Since this zone does not exist in the 3D case, the heating remains high. A recirculation zone does exist in both 20 m simulations, so they both see the cooling effect near the axis.

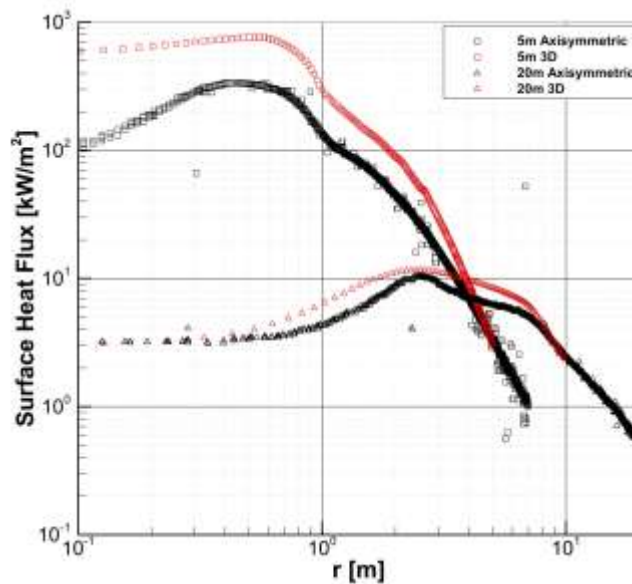


Fig 6: LMDE plume surface heating at 20 m and 5 m altitudes – axisymmetric vs. 3D DAC results.

Although the 3D half symmetry DAC models tend to overpredict surface heat flux, especially at the 5 m altitude, they can be considered conservative, and hence sufficiently validated for this preliminary study. The lander engines never reach altitudes lower than 10 m from the ground [7] and are significantly smaller than the LMDE so the stronger validation at 20 m altitude is likely more relevant. If higher accuracy surface heating predictions are desired, additional time could be spent trying to reduce the cell sizes along the ground in the 3D case. This is evident because in a grid sensitivity check, the surface heating values were found to still be decreasing toward the 2D solution with the current cell sizes.

V. LANDER ENGINE DSMC SIMULATIONS

The DAC simulations used to model engine plume of the potential lander are staged such that the grid can be manually adjusted based on density. A 2D axisymmetric ‘Nearfield’ stage receives inflow data from the CFD solution and extends only a few meters from the nozzle exit. It has a 0.5 mm grid to resolve the highly collisional flow near the nozzle. Then flow data from this Nearfield solution is used as the inflow boundary for a ‘Farfield’ 3D stage that extends to the ground, and further outward from the nozzle axis. This transition to 3D is necessary since the engines are canted from vertical and require at least a half-symmetry simulation. Since the Farfield grid is generally very coarse, smaller wall cells are added along the ground such that accurate heat rates can be computed.

The CFD/DSMC interface, as mentioned earlier in Section III, is first sketched as far out from the nozzle as possible, based on the STAR-CCM+ contour plots of Knudsen number, with velocity streamlines. Then the normal velocities are calculated along the interface to determine if it is supersonic everywhere. If not, then the interface is moved closer to the exit plane, as needed. The interface eventually evolves into a straight line interface extending from the outer edge of the nozzle to the axis, 0.1 m downstream of the nozzle exit plane. This interface can be seen in Figure 7.

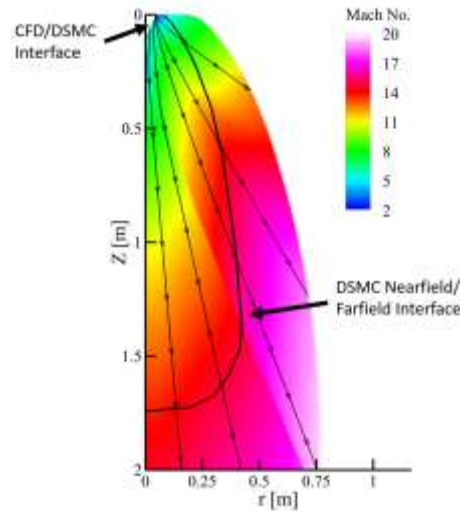


Fig 7: Axisymmetric Nearfield stage Mach number from DAC simulation, with CFD/DSMC and Nearfield/Farfield Interface locations shown. Nozzle exit plane is located at $Z = 0$ and nozzle axis is Z -axis. CFD data is blanked out in this figure.

To transition from the 2D Nearfield simulations to the 3D Farfield simulations, another interface definition is required. Using an axisymmetric contour plot of number density in the domain of Figure 7, a boundary is sketched along an isocontour to obtain an interface. This interface, shown in Figure 7, extends approximately 1.75 m from the nozzle exit, which is considered to be well within the domain that can be considered axisymmetric given that the lowest altitude to be studied is 10 m. The interface-normal flow is again verified to be supersonic, which it easily is. This is the case because this interface is much further out from the nozzle than the CFD/DSMC interface, where the flow has greatly accelerated and is not so sensitive to the orientation of the boundary. This boundary is then swept across 180 degrees to form the required 3D inflow interface for the Farfield simulations. For the extremely large domain simulations at an altitude of 15 m and higher, a second 3D Farfield stage is required in order to transition to an even larger uniform grid. The transition interface to this second Farfield stage is shown in Figures 8 and 9 and is approximately 7 m downstream from the nozzle exit. Cells as small as reasonably possible are still used near the ground to resolve the surface shock and get an accurate prediction of surface heating.

The descent stage of the potential Europa Lander is assumed to use four pairs of engines for landing. Each pair consists of one engine canted at 5 degrees and one canted at 30 degrees. During the first part of powered descent, above 30 m, all eight engines are used to decelerate. Below that, only the 30-degree canted engines are used to minimize plume contamination of the landing site and Lander, which is lowered from underbelly of the descent stage via Sky Crane until it contacts the ground at an altitude of 12 m [7]. Ultimately, it would be necessary to model engines in pairs to capture the complex interactions between their plumes, an established DAC capability demonstrated in e.g. Lumpkin et al. [1,2,9]. However, for this preliminary exercise, only a single engine was modelled in each simulation to get a first order idea of what the plume environment is without requiring more complex 3D CFD modelling.

DAC plume simulations are performed at altitudes roughly enveloping the final stage of the descent profile for a potential Europa Lander mission. Plumes are simulated on nozzles canted 30 degrees at altitudes of 25 m, 20 m, 15 m and 10 m. A 5-degree canted nozzle is also modelled at 25 m only. The resulting pressure fields for the 25 m (5° cant and 30° cant) and 10 m (30° cant) altitudes in the plane of symmetry are shown in Figure 8, 9 and 10, respectively. The nozzle is canted from vertical (y-axis). No recirculation zones are observed in these canted nozzle simulations, as was seen with the LMDE plume, even in the 5°-cant case which is pointed nearly straight down.

At an altitude of 25 m and cant of 5°, as shown in Figure 8, the surface shock is almost parallel to the ground, with a thickness of ~2 m. It starts veering upward approximately $r = -5$ m in one direction and at around $r = +10$ m in the other direction. When the nozzle cant is increased to 30°, the surface shock becomes more angled with respect to the ground and its minimum thickness decreases to ~1.5 m, approximately +3 m from the cant axis. The shock remains flat all the way out to ~22 m where it starts veering upward at a higher angle. At a lower altitude of 10 m, with the same cant of 30°, the minimum surface shock thickness remains the same at ~1.5 m, but moves inward toward the cant axis to $r \sim 1$ m. It stays roughly parallel to the ground out to about $r = +12$ m. The r - locations where the surface shocks start to divert upward tend to be approximately where the reflected nozzle shock intersect them. This is consistent with what is seen in the LMDE validation case.

In Figure 11, Mach number contours more clearly show the acceleration of the nozzle flow up to the surface shock, the shock thickness and resulting subsonic region downstream of the shock. As altitude and cant decrease, the flow reaches a lower velocity just upstream of the shock since it has less distance to accelerate. For the 30° canted cases, at 25 m, the flow accelerates to Mach 40, however, at 10 m, the flow only accelerates to Mach 27. Similarly, but to a lesser extent, when the nozzle cant is decreased to 5° in the 25 m case, the flow accelerates to only Mach 37. The shock thickness also decreases with decreasing altitude. In all simulations, downstream of the shock in the subsonic region, the flow is redirected in the radial direction along the surface.

The 10 m, 15 m and 20 m altitude cases are solved using a 2.5 cm uniform grid, with 1.25 cm cells along the ground. This is a grid very similar to the one used in the validation problem. The results for the 25 m altitude case are solved using a 5 cm uniform grid due, with no wall cells, due to the larger required domain size. A grid sensitivity check for each case shows surface pressure to be converged well. However, surface heat flux is still dropping with each reduction of grid size, suggesting the reported values represent a slight overestimation. The cell sizes exceed the mean free path in the majority of the plume core, however are small enough to resolve the gradient scale lengths of macroscopic flow properties throughout.

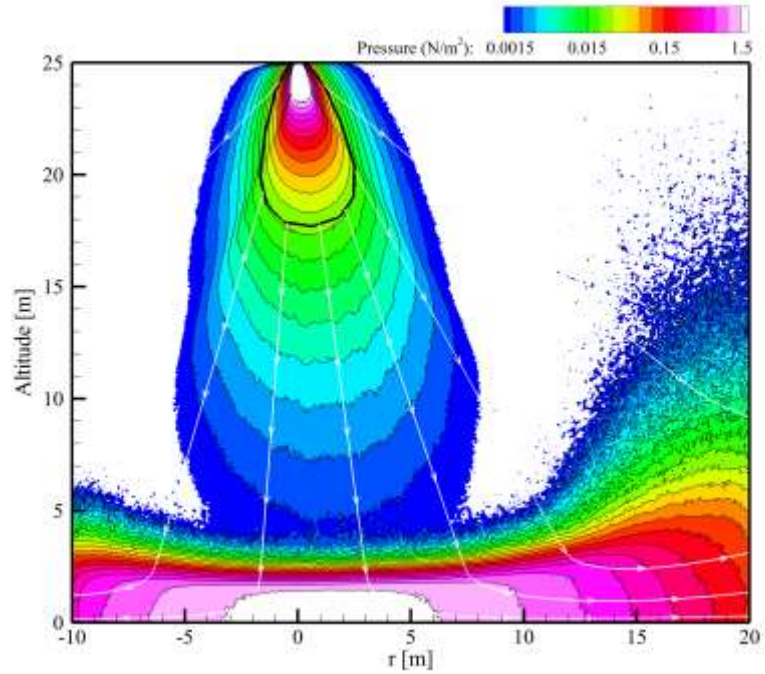


Figure 8: Pressure contour for 5° canted engine at 25 m altitude, using 5 cm uniform grid. CFD and DSMC Nearfield data is blanked out. Second Farfield inflow interface is shown by solid black line.

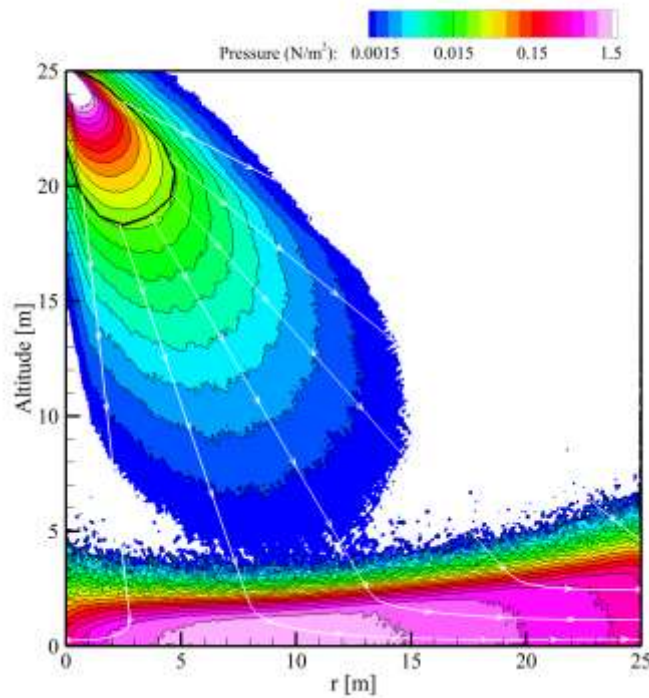


Figure 9: Pressure contour for 30° canted engine at 25 m altitude, using 5 cm uniform grid. CFD and DSMC Nearfield data is blanked out. Second Farfield inflow interface is shown by solid black line.

[Type here]

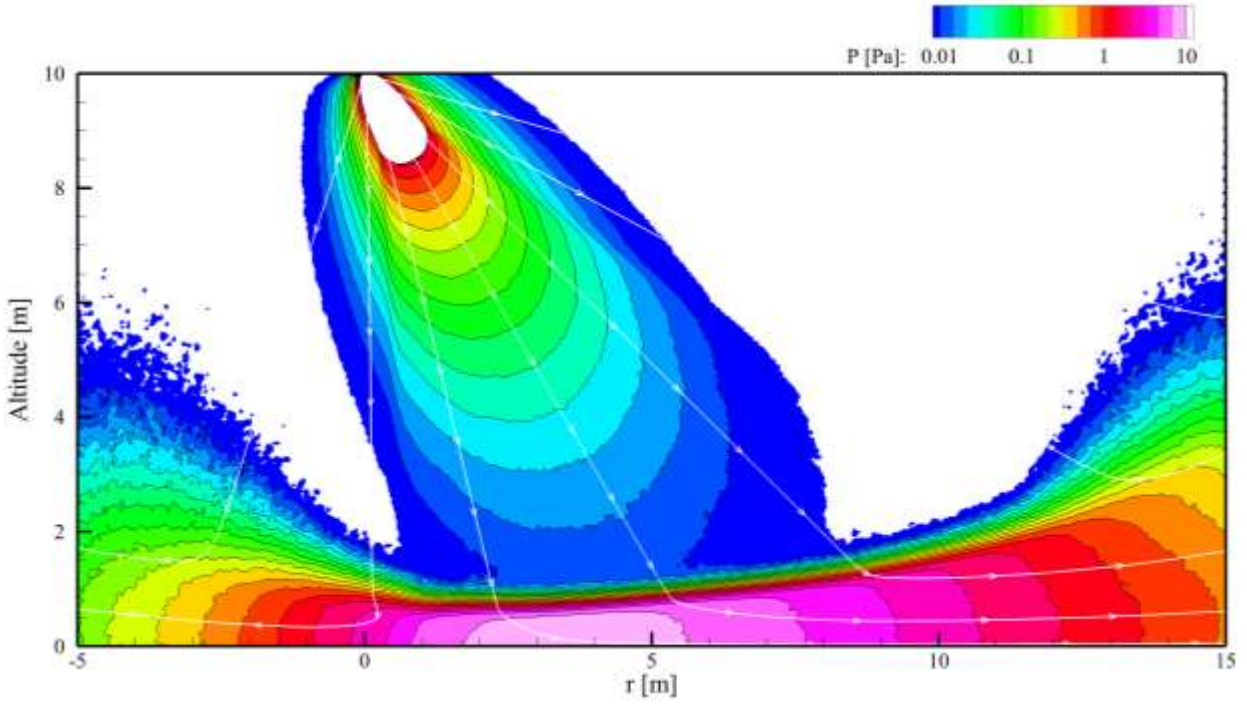


Figure 10: Pressure contour for 30 degree canted engine at 10 m altitude

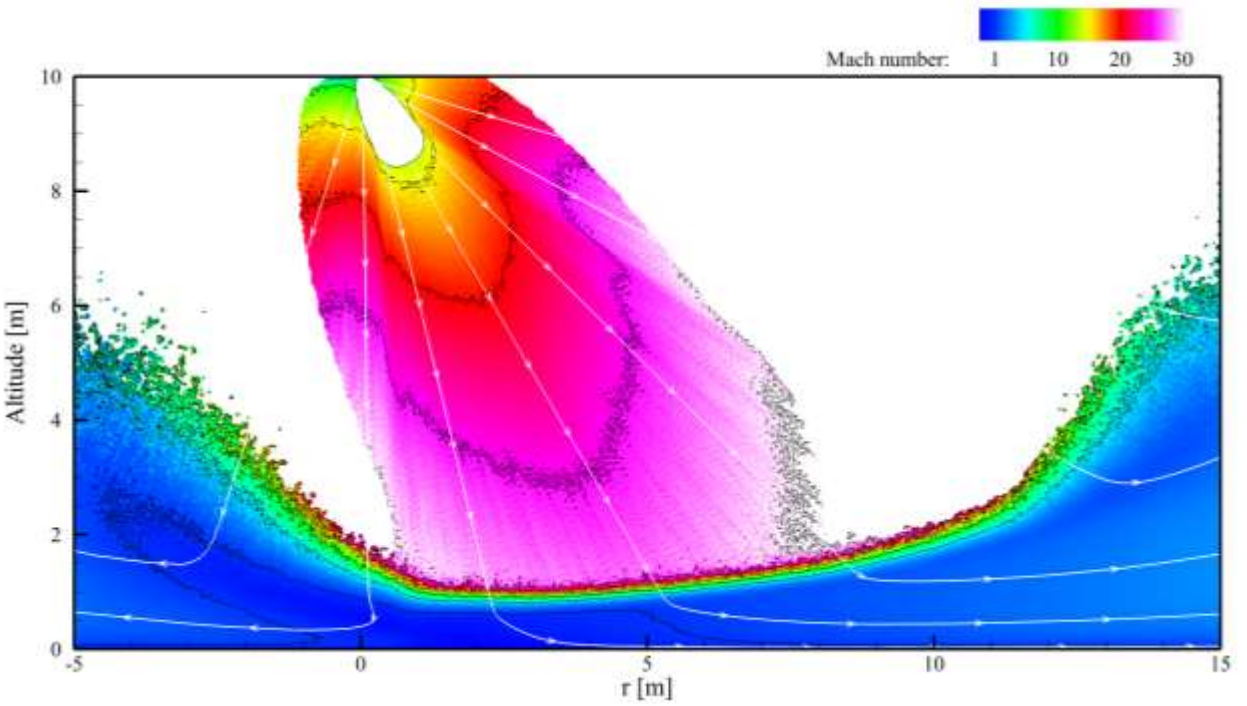


Figure 11: Mach number contour for 30 degree canted engine at 10 m altitude

[Type here]

The half symmetry ground pressure contour is shown in Figure 12. The plane of symmetry intersects this contour at the r-axis. Contours for heat flux and NH_3 n-flux are similar in nature. Profiles along the plane of symmetry (at $y = 0$) are the maximum and hence most conservative values. Surface profiles for heat flux, pressure and ammonia (NH_3) number density flux (n-flux) along the plane of symmetry are shown in Figure 13. For a given altitude, peak pressure and n-flux occur at the same radial location, slightly outboard of peak heat flux, and less so with decreasing altitude. The magnitude of all three parameters increases as the lander descends. At the lowest altitude of 10 m, a peak heating value of 2.65 kW/m^2 occurs at a radial distance of about 3.3 m. A peak pressure of 8.6 Pa and a peak n-flux value of $1.36\text{E}+23$ molecules/ m^2/s occur at a radial distance 3.5 m. At a constant altitude of 25 m, the 5° canted nozzle has a slightly higher peak heating, pressure and n-flux than the 30° canted nozzle. Its peaks are within 1 m of the cant axis and do not taper off much at all near the axis and due to the absence of a cooling recirculation zone.

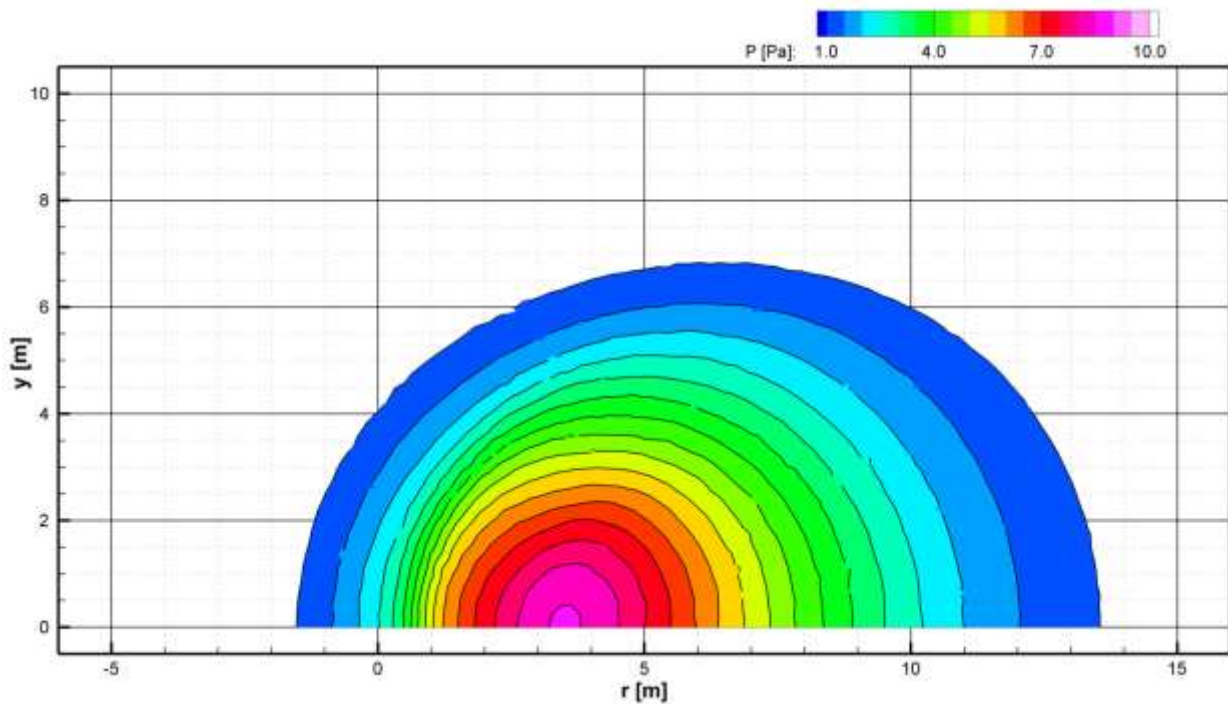


Fig. 12: Ground surface pressure contours for 10 m altitude. Plane of symmetry is along r-axis.

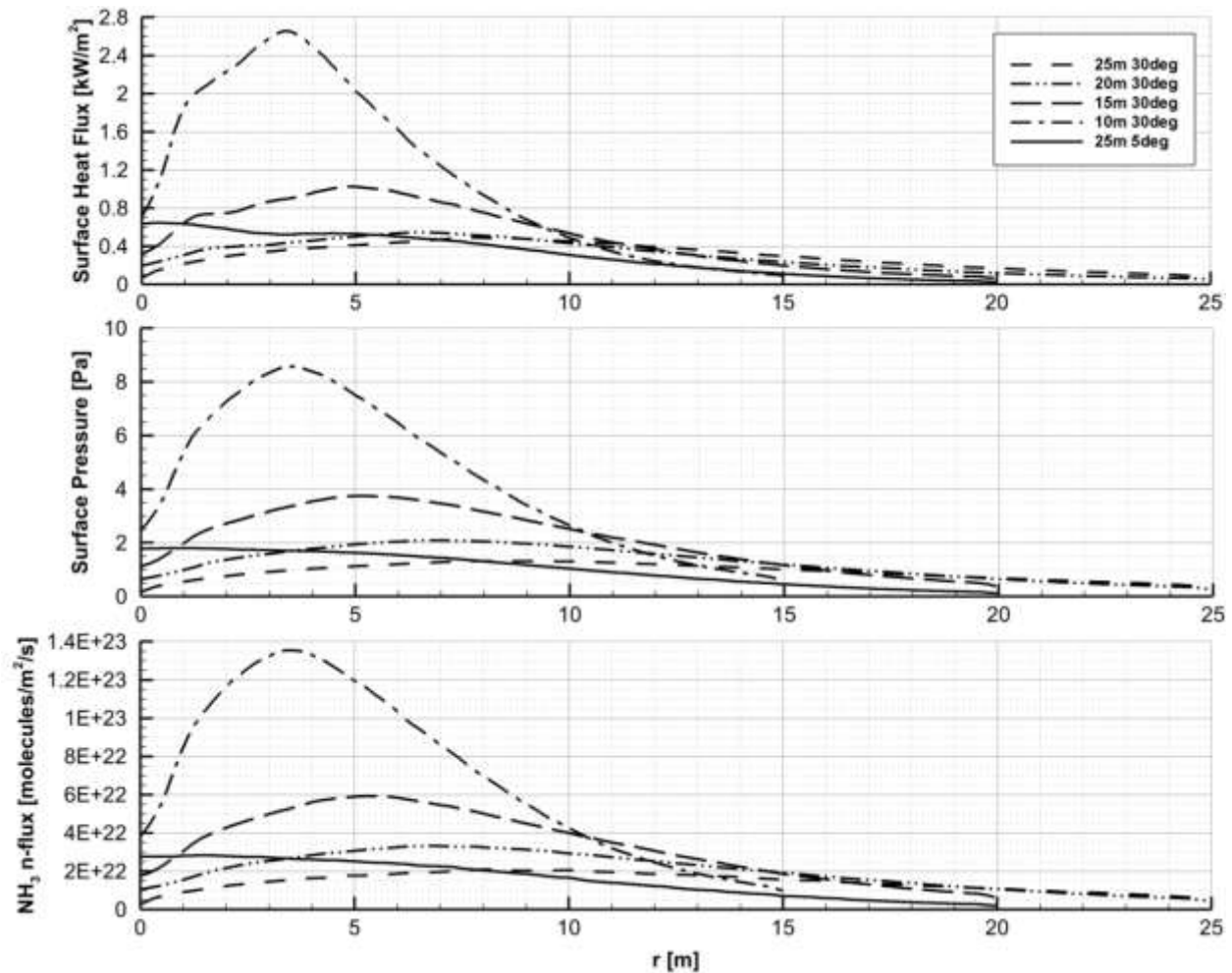


Figure 13: Surface heat flux, pressure and ammonia number density flux for all DAC simulations

Time-dependent profiles of the flow parameters can be approximated given the altitude-versus-time profiles of the vehicle to compute total ammonia accumulation and surface erosion over the landing area. Additionally, pressure and velocity fields can be passed on to entrainment models to assess how the surface particles are redirected upward toward the vehicle during landing. Lastly, the lander vehicle itself can be added to the model to study the direct impingement of the plume onto the lander body or specific instruments to address dynamics, heating or contamination concerns. Approximations can be made using the plumes of single engines, however, it is also important to study the complex flow fields resulting from the interaction of nozzle pairs, which can augment the effects of plume impingement [2].

VI. CONCLUSION

STAR-CCM+ is used to solve the axisymmetric plume flow field inside and just downstream of a potential Europa lander nozzle, where the continuum assumption is valid. A CFD/DSMC interface is established within this continuum region, based on Knudsen number and interface-normal Mach number. Then flow data is manually passed to the DSMC code where the plume flow is modelled all the way to the Europa surface in 3D, at altitudes spanning the final stages of descent of a potential Europa Lander mission.

The staged use of STAR-CCM+ and DAC codes is validated successfully with a lunar descent engine simulation. The use of temperature dependent specific heat values in the CFD domain, consistent with the validation problem, is essential to reproduce accurate results in the entire domain. The flow field pressures produced by DAC are validated well but the 3D simulations conservatively overpredict heat flux at the surface due to the overly coarse cell size used. Additionally, surface cooling recirculation zones in line with the nozzle axis are observed in the axisymmetric cases and in the higher altitude 3D case.

Half symmetry 3D plume simulations of 30-degree and 5-degree canted nozzles at relevant altitudes show flow expanding away from the nozzle, reaching speeds of Mach 27 to Mach 40 before being decelerated across a surface shock and redirected along the ground. This surface shock becomes wider, closer to the ground at its nearest point and more angled with respect to the ground as the cant angle increases. As altitude decreases, for a 30-degree cant, the surface shock does not get any closer to the ground at its nearest point but the nearest point moves inward radially toward the cant axis. No surface cooling recirculation zones are observed in these canted simulations.

Maximum heat flux, pressure and NH_3 n-flux occur at the plane of symmetry on the surface. A maximum surface heat flux of 2.65 kW/m^2 occurs 3.3 m from the nozzle cant axis at the lowest altitude of 10 m. A peak pressure of 8.6 Pa and a peak n-flux value of $1.36\text{E}+23 \text{ NH}_3$ molecules/m²/s are observed just outward from this at 3.5 m from the nozzle cant axis.

With the data produced in this study, more detailed time dependent analyses can be carried out to assess the accumulation of NH_3 on the surface, the erosion of the surface and entrainment of surface particles given the altitude-versus-time profiles of a potential lander and the full 3D data set. Additionally, the decent stage, lander or any other body of interest can be added to the model to study the impingement of the plume on specific surfaces.

Furthermore, the methodology developed in this study can be applied to future icy moon missions and any mission with similarly low background pressure.

ACKNOWLEDGEMENTS

The research was carried out at the Jet Propulsion Laboratory, California Institute of Technology, under a contract with the National Aeronautics and Space Administration.

Copyright 2019 California Institute of Technology. U.S. Government sponsorship acknowledged.

The decision to implement the Europa Lander will not be finalized until NASA's completion of the National Environmental Policy Act (NEPA) process. This document is being made available for information purposes only.

We would like to thank J. Morgan Parker (JPL) for Europa Lander project leadership support. We would like to thank Dr. Aaron Morris (Purdue University) for having substantial discussions with the team pertaining to his work. We would also like to thank Drs. Jonathan Burt (NASA), Iain Boyd (University of Michigan, Ann Arbor), David Goldstein (University of Texas at Austin) and Forrest Lumpkin (NASA) for helping with CFD and DSMC methodology. We would like to acknowledge Carlee Wagner (Siemens) for STAR-CCM+ and Dr. Benedicte Stewart (NASA) for DAC support.

Simulations were carried out on supercomputers maintained by JPL and the Texas Advanced Computing Center.

VII. REFERENCES

1. Morris, A., 2012. "Simulation of Plume Impingement and Dust Dispersal on the Lunar Surface," Ph.D. Dissertation, Aerospace Engineering Dept., Univ. of Texas at Austin, Austin, TX.

[Type here]

2. Morris, A., Goldstein, D., Varghese, P., and Trafton, L., 2015. "Lunar Dust Transport Resulting from Single- and Four-Engine Plume Impingement," *AIAA Journal*, Vol. 54, No. 4, pp. 1339–1349.
3. Morris, A., Goldstein, D., Varghese, P., and Trafton, L., 2015. "Approach for modeling rocket plume impingement and dust dispersal on the Moon," *Journal of Spacecraft and Rockets*, Vol. 52, pp. 362–374.
4. Lorenz, Ralph D., 2016. "Lander rocket exhaust effects on Europa regolith nitrogen assays," *Planetary and Space Science*, Vol. 127, pp. 91-94.
5. Plemmons, D.H., Mehta, M., Clark, B.C, et al., 2008. "Effects of the Phoenix Lander Descent Thruster Plume on the Martian Surface," *Journal of Geophysical Research*, VOL. 113, E3.
6. LeBeau, G.J., 1999. "A Parallel Implementation of the Direct Simulation Monte Carlo Method," *Computer Methods in Applied Mechanics and Engineering*, Vol. 174, Nos. 3–4, pp. 319–337.
7. Hand, K.P., Murray, A.E., Garvin, J.B., Brinckerhoff, W.B., Christner, B.C., Edgett, K.S., Ehlmann, B.L., German, C.R., Hayes, A.G., Hoehler, T.M., Horst, S.M., Lunine, J.I., Nealson, K.H., Paranicas, C., Schmidt, B.E., Smith, D.E., Rhoden, A.R., Russell, M.J., Templeton, A.S., Willis, P.A., Yingst, R.A., Phillips, C.B., Cable, M.L., Craft, K.L., Hofmann, A.E., Nordheim, T.A., Pappalardo, R.P., and the Project Engineering Team (2017), Posted February 2017. "Report of the Europa Lander Science Definition Team."
8. Boyd, I.D., 2003. "Predicting Breakdown of the Continuum Equations Under Rarefied Flow Conditions," CP663, *Rarefied Gas Dynamics: 23rd International Symposium*, American Institute of Physics 0-7354-0124.
9. Lumpkin, F., Marichalar, J., and Stewart, B., 2012. "High Fidelity Simulations of Plume Impingement to the International Space Station," 33rd JANNAF Exhaust Plume and Signatures Subcommittee Meeting, Monterey, CA, Abstract No. 2012-0004AD.